Hindawi
International Journal of Aerospace Engineering
Volume 2020, Article ID 8503194, 10 pages
https://doi.org/10.1155/2020/8503194

Research Article

Buckling Instability of Flexible Joint under High Pressure in Solid Rocket Motor

Wang Chunguang,[1] **Xu Guiyang**,[2] **and Gong Jianliang**[2]

[1]*College of Electrical and Control Engineering, Shaanxi University of Science & Technology, Xi'an 710021, China*
[2]*Xi'an Modern Chemistry Research Institute, Xi'an 710065, China*

Correspondence should be addressed to Wang Chunguang; king19850723@163.com

Received 20 June 2019; Revised 27 August 2019; Accepted 7 October 2019; Published 4 January 2020

Academic Editor: Marco Pizzarelli

Deflection torque decrease of flexible joint under increasing pressure was normally attributed to the changing shear stress and has not been carefully resolved, which was far from convincing. To systematically investigate the mechanism, the structure characteristics of the flexible joint were analysed under different pressures. It was found that the decrease in deflection torque of the flexible joint was mainly due to the buckling response when it bears the deflection and pressure at the same time. The Riks method was utilized in this paper with the simulation of the buckling process of the flexible joint by ABAQUS. The static Riks method and general method were applied, respectively, to simulate the different pressurization processes at different pre-angles to obtain the rules of swing angle changing with pressure. The spring torque under various pressures was obtained and had a good coherence with the test results. For industrial applications, the concept of container pressure torque and its formula were proposed in this study, which was demonstrated to be of high accuracy. The simulation method and conclusions in this paper will definitely provide the beneficial reference to the design of the flexible joint in high-pressure working environment.

1. Introduction

The thrust vector control of solid rocket motor is mainly based on deflecting nozzle, gas helm, and secondary jet, among which deflecting nozzle has minor effects on engine efficiency and is capable of direction control for a long period. Deflecting nozzle could be divided into flexible nozzle, bean nozzle, and ball-socket nozzle, and flexible nozzle is widely utilized in solid rocket motor due to its simple structure and mature fabrication technique. Flexible joint connects and encapsulates the movable components with the fixed parts of the flexible nozzle, which is one of the key components in thrust vector control system of solid rocket motor. In the practical application of the flexible joint, the decrease of the spring torque usually leads to the swing torque drop as the working pressure increases, which widely exists in different kinds of motors. When the working pressure reaches a critical value, the deflection torque will generally approach zero or even negative, resulting in the instability of the flexible joint and adversely affecting the thrust vector control [1, 2]. In the flight process, the missile needs to change the thrust direction by swinging the swing nozzle. Therefore, it is necessary to study the reason of the reduction of the swing torque of the flexible joint under high pressure, so as to accurately predict the swing torque under different combustion chamber pressures.

Researchers have paid close attention to the design of flexible joints and their mechanical response during high-pressure work, and lots of analysis have been made on the structural reliability, strength, and stability, along with some conclusions [3–10], which provide a very useful reference for the design of flexible joints. However, few studies have been devoted to the internal reasons for the reduction of the deflection torque when the flexible joints are under high pressure.

At present, the teaching textbook for practical engineering applications in China simply attributed deflection torque decrease of the flexible joint under high pressure

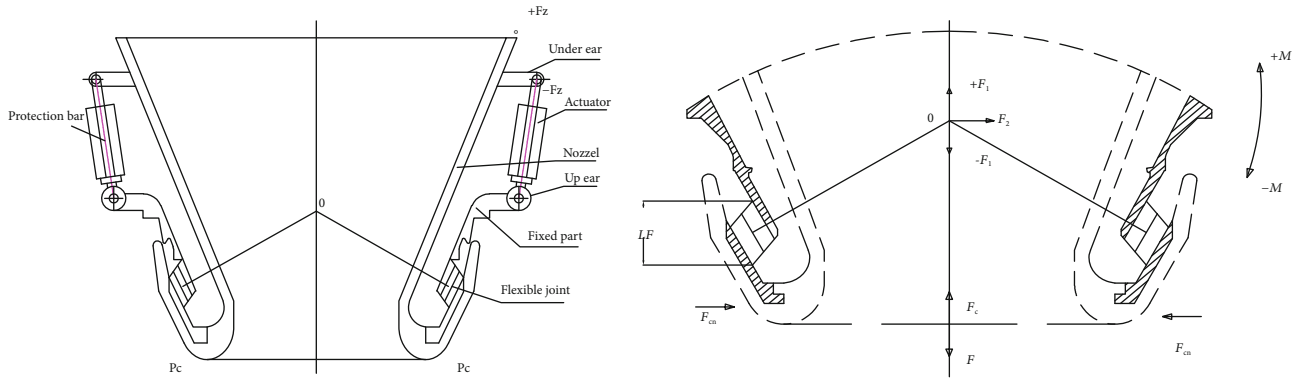

Figure 1: The mounting position and force form of the flexible joint in the nozzle.

to the reduction of shear modulus in elastic rubber materials [1]. In [1], the calculation method of deflection torque was shown.

$$\frac{M_t}{\theta} = \frac{2.094 \times 10^{-2} G {\rho_0}^3 {\rho_i}^3}{{\rho_0}^3 - {\rho_i}^3} (I(\beta_2) - I(\beta_1)). \quad (1)$$

However, X. K. Wang et al. and W. Chunguang et al. [11, 12] designed the biaxial loading test device and triple/quadruple pieces in order to obtain the elastic modulus of flexible joints with shear stress changes with the pressure. The specimens were subjected to compression-shear loading test and finite element numerical simulation, which indicated the small change of the shear modulus of the rubber material with pressure.

In order to study the mechanism of the spring torque reduction of flexible joint with the increasing pressure, Wang et al. [2] utilized the finite element model that simulates the swinging process of the flexible joint. The shear stress distribution on the elastic part was calculated with pressure change and was concluded to be the inherent reason for the reduction of spring torque. In this paper, the analysis shows that the distribution of shear stress on the elastic part is not the root cause of the deflection torque reduction of the flexible joint with the pressure change. Because of the high pressure and swinging of the flexible joint, the whole configuration produces a response to the external force, which results in the change of the shear stress distribution on the elastic component and eventually leads to the reduction of the spring torque. Response serves as a precondition, and then shear stress distribution changes, eventually leading to variations in spring torque. This response is the buckling of the flexible joint under the combined effect of high pressure and swinging.

Buckling analysis is mainly used to study the stability of structures under certain loads and to determine the critical loads for structural instability, which mainly includes linear elastic buckling and nonlinear buckling analysis. Linear elastic buckling analysis is also called eigenvalue buckling analysis, while nonlinear buckling analysis includes geometric nonlinear instability analysis, elastic-plastic buckling analysis, and nonlinear postbuckling analysis [13]. In nonlinear buckling analysis, the Riks method is one of the most stable, computationally efficient, and reliable iterative control methods [14, 15].

Based on the classification of buckling, this study analyzes the characteristics of buckling response of flexible joint structure. Through the static general and static Riks modules in ABAQUS, the calculation of the swinging process of the flexible joint was carried out. The simulation results were compared with the experimental data to analyze the buckling response of the flexible joint structure under high pressure and swinging. In order to facilitate the engineering application, the concept of container pressure torque and its calculation formula of the torque are proposed. The excellent accuracy of calculation formula was demonstrated by the experimental data and can provide useful reference for the design of flexible joints.

2. Working Processes and Structure Characteristics of Flexible Joints

The installation form of the flexible joint in the flexible nozzle is shown in Figure 1, and the core component is a flexible joint. During the working process of the motor, the shear deformation of the flexible joint is realized by the expansion and contraction of the actuator, thereby realizing the swing of the flexible nozzle and realizing the change of the thrust direction of the motor. Figure 1 shows the mounting position and force form of the flexible joint in the nozzle. Figure 2 is a shear deformation process of a flexible joint.

During model development, every flexible joint must be tested for their cold swing performance on the ground, simulating different pressures in the combustion chamber. The flexible joint was placed in the position as shown in Figure 3. In this scheme, the joint is installed above the container within which the pressure is variable. The rigid pendulum is used to represent the expansion section of the nozzle. The actuator is installed between the points B and C to apply the swing torque.

The flexible joint is composed of a plurality of concentric ring-shaped spherical elastic parts and reinforcing ones alternately bonded with each other, with a flange at both ends of the joint. The elastic components are mainly made of natural rubber or silicone rubber, while the reinforcing ones are

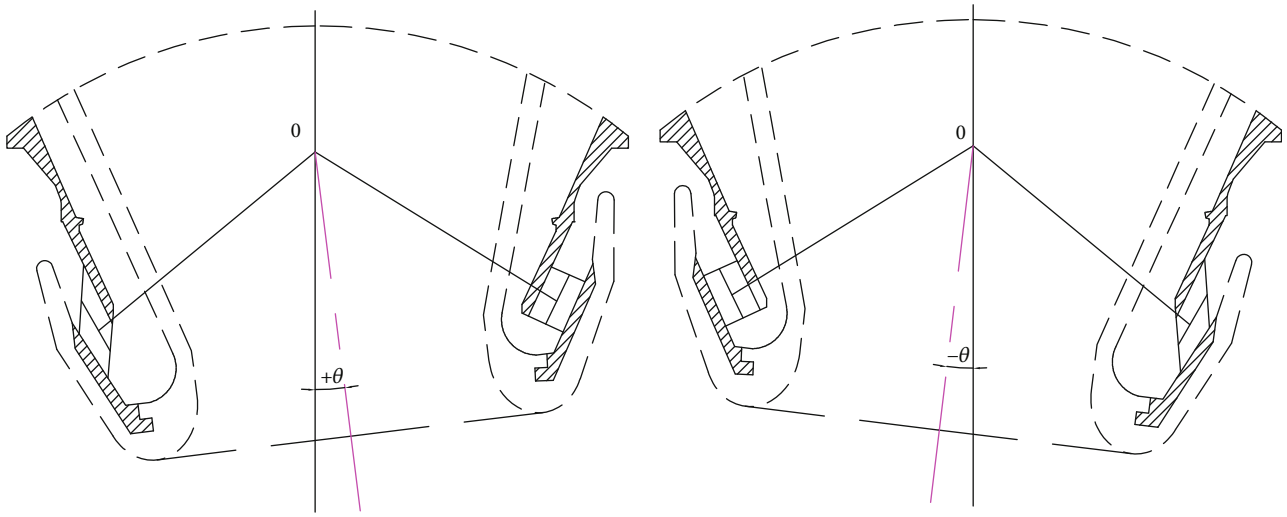

Figure 2: Shear deformation process of a flexible joint.

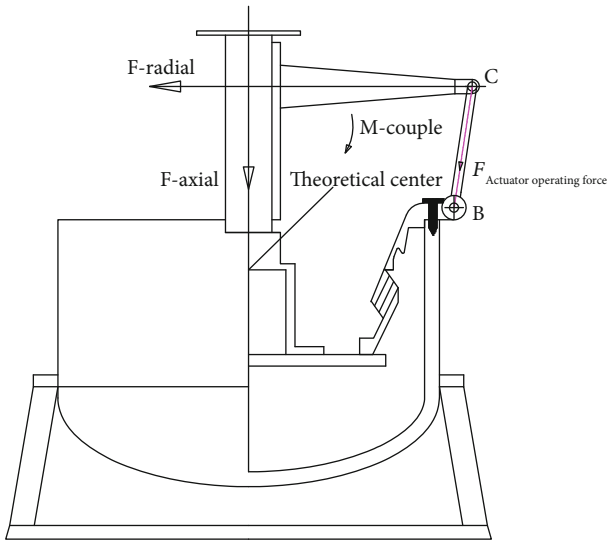

Figure 3: The swing test diagram of flexible joint.

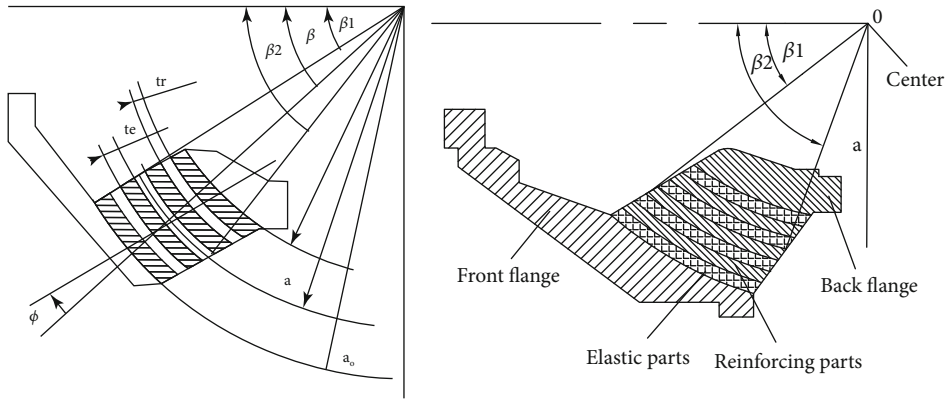

(a) Parameters of flexible joints

(b) The various components of flexible joints

Figure 4: Flexible joint structure.

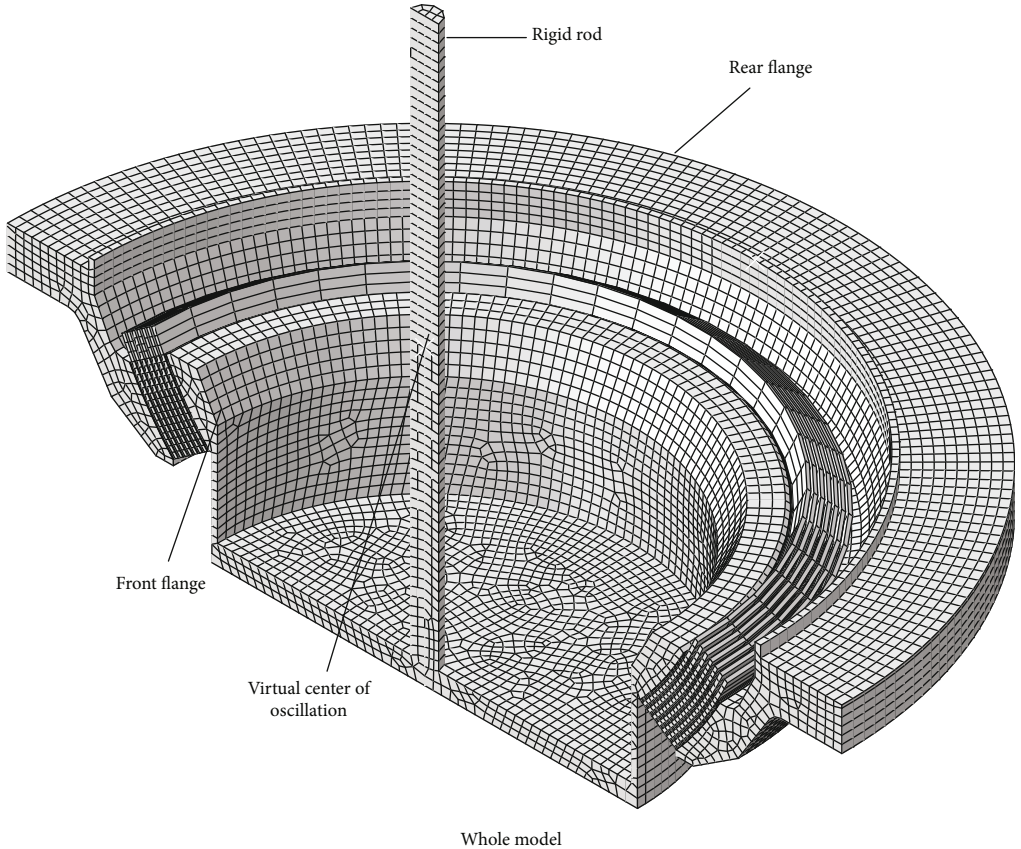

Figure 5: Flexible joint computing model.

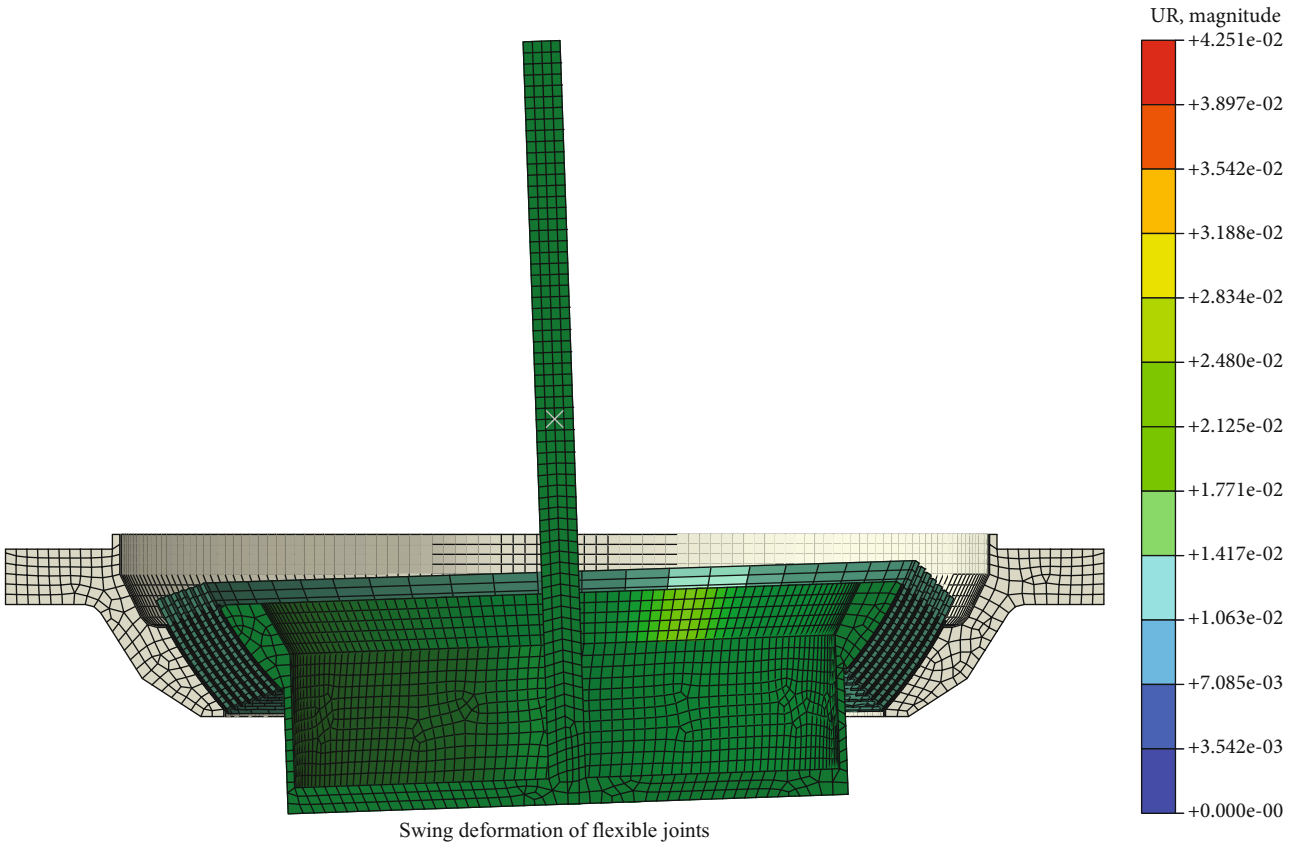

Figure 6: Calculated deformation diagram.

composite materials, metals or carbon fibers. The specific structure of the flexible joint is shown in Figure 4.

The flexible joint was designed as a nonlinear rubber stack structure, and the swing process is shown in Figure 3. The actuator shrinks or elongates to apply a deflecting torque. Operating force of the actuator was passed through the pendulum (nozzle structure of the actual motor) to the front flange of the flexible joint, in order to achieve flexible joint swinging. Under internal pressure, the flexible joint was subjected to both internal pressure and the swing torque at the same time. The experimental results illustrated that the deflection torque reduction mainly resulted from the decrease of the spring torque of the flexible joint when it was compressed in the axial direction, which is widely observed in several models. The sensitivity of the pressure is not exactly the same, based on changes of the rubber materials and flexible joint size.

Two methods are commonly used to predict the critical buckling load and the structure shape after buckling: eigenvalue (linear) buckling analysis and nonlinear buckling analysis. Eigenvalue buckling analysis is linear analysis of the structure, which is used to predict the theoretical buckling strength of ideal linear elastic structures. However, due to the special structure of the flexible joint and the super-elastic rubber material, the buckling process of the joint under the dual roles of pressure and swinging

should be nonlinear. Nonlinear buckling analysis generally consider the initial defects of structures, such as one thousandth of length (for the stability of the beam with axial compression load), one tenth of the wall thickness (for the stability of the case with the external load), fabrication error in the actual production, or the initial disturbance of external forces.

The analysis shows that the buckling process of the flexible joint is similar to that of the rubber stack [16]. The deflection torque of the joint is equivalent to the initial disturbance of the lateral force, resulting in a certain angular displacement of the joint. Under increasing pressure, same torque is able to produce greater angular displacement in this way. In particular, the lateral deflection torque and the pressure are loaded, respectively. Through the presimulation and experimental verification, the loading order of the two has little effect on the reduction of the spring torque. The process above is also called the instability process of flexible joints.

3. Numerical Calculation Model and Calculation Process

The calculation model in this study is established based on the literature [2]. As shown in Figure 5, the pressure load is directly applied to the front flange and the plugging cover to achieve the simulation of different experimental container pressures. The driving load is realized by applying torque at the virtual center point of swinging, which is connected with the front flange through the rigid rod. The rubber material is simulated using a super-elastic constitutive model, and the reinforcing component is assumed to be steel materials. 18,000 units are established in the model, which consists of 8 layers of elastic parts and 7 layers of reinforcing components. The model is divided into 25 equal parts in the circumferential direction and 15 equal parts in the width direction. The thickness direction is divided into 1 layer to 3 layers. Elastic rubber components are simulated using hybrid C3D8H unit, while the reinforcing ones use the reduction integral C3D8R unit. The flanges at both ends, the pressure cover, and the loading part could be seen as rigid bodies, which is simulated via the usage of rigid body R3D4 unit [2].

The displacement constraint $W = 0$ is applied to the z-axis of the symmetry plane and the rear flange is fixed. The center of gravity has the freedom of translation U_1 and U_2 and freedom of rotation U_3.

The calculation condition has two steps.

Step 1. The flexible joint is pretilted at a certain angle, and the driving load is obtained by applying a rotational displacement at the virtual center of gravity, which is connected to the front flange through a rigid rod. This is equivalent to the initial disturbance or the initial defect of the joint structure.

Step 2. Directly apply pressure load to the front flange and cover to achieve simulation of different experimental container pressures, which has a maximum value of 6 MPa (maximum pressure of the actual motor combustion chamber). For Step 2, two methods (static general and static Riks) are used for calculation.

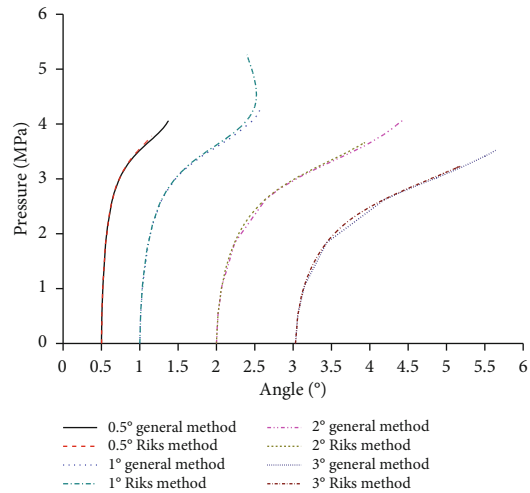

Figure 7: Pressure and swing angle curve.

4. Comparative Analysis of Simulation Results and Experimental Data

Calculation results based on two different methods above are shown in Figure 6(a). The joint was initially swung 1°. The swing angle gradually increased to 2.435°, with the pressure increasing and the spring torque reducing. When the pressure is close to 6 MPa, the grid of elastic rubber component is distorted and the calculation is forced to stop. The partial grid deformation is shown in Figure 6(b).

The swing angle changes under different pressures were calculated when the preswing angle was set at 0.5°, 1°, 2°, and 3°, respectively, and the maximum pressure is set to 6 MPa. The results were drawn as a curve and are shown in Figure 7. As you can see from the graph, the data got from the general static method is with a slightly higher calculation capacity of pressure and is very close to that from the Riks method.

In nonlinear buckling analysis, the instability point and instability processes of structures are usually judged by observing the load displacement curve. The load displacement curve of the structure mainly follows three forms, as shown in Figure 8. The solid line in the figure represents a stable equilibrium path, while the dash line represents an unstable one. P_c is the critical load. Based on the change of load displacement path, buckling can be further divided into extreme buckling, stable and unstable branch buckling.

Comparing the three curves, the buckling processes of the flexible joint is closer to the stable buckling process in Figure 8(b) without showing any clear critical load. The analysis shows that this is mainly due to the special nonlinear structure of the flexible joint. With the increase of pressure, the swing angle of the structure increases, which indicates the simultaneous shape change of the joint structure. For the deformation analysis of the static structure, the deformation is usually very large. The later step is determined directly by the deformation of the previous step, so the critical load for the previous step should also change momentarily, as the slope of the curve does all the time.

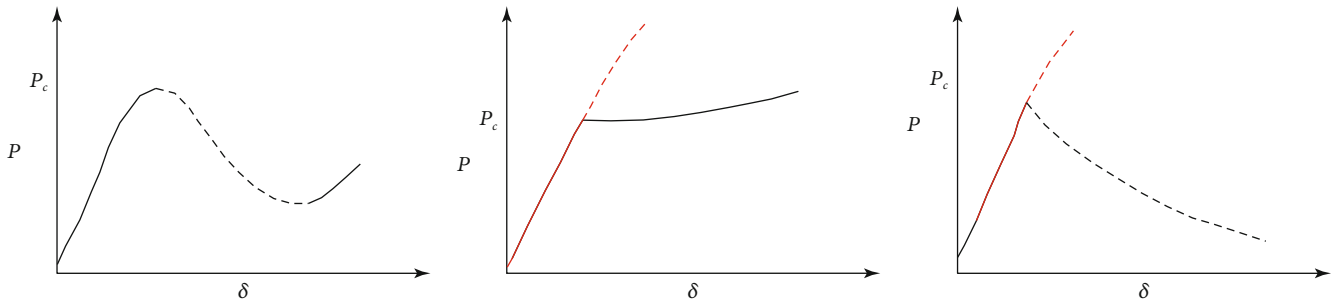

(a) Extreme buckling (b) Stable branch buckling (c) Unstable branch buckling

Figure 8: Load and displacement curves under different conditions.

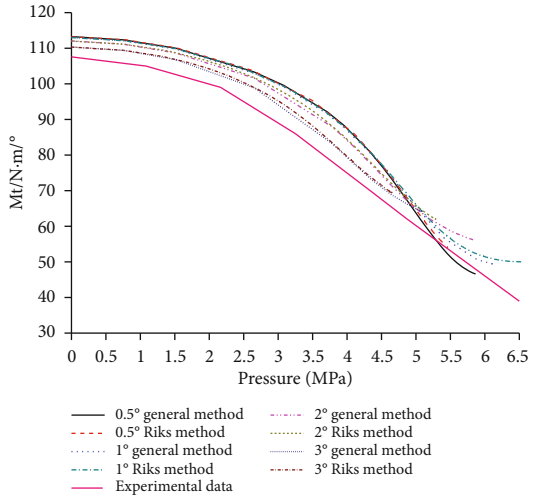

Figure 9: The spring torque changes with the pressure.

Besides, the slope of different curves change more obviously as the pre-swing angle increases, indicating the larger structural instability. The reason behind that is the increase of lateral disturbance due to the preswing angle increases, which leads to the larger increase of swing angle under the same pressure; and thus, the structure is more prone to serious instability.

We also calculated the spring torque by the two methods under different pressures. To compare the data with the experimental results, the trend of the spring torque is illustrated in Figure 9.

It can be seen from Figure 9 that the trend of spring torque calculated by general and Riks methods are almost the same. Compared with the experimental results, the numerical results agree with the experimental results showing very small error level. However, the downward trend of the spring torque from the experimental results is more obvious than the numerical calculation. The main reason for the difference is that the finite element model did not take the manufacturing variations in the actual production of flexible joints into account, such as the unevenness of the thickness of the elastic components and the reinforcing ones. The dimensional errors in the actual production may become part of the initial disturbance, which leads to easier deflection of the joint and faster drop of the spring torque. At higher pressure, the rubber units endure a larger deformation and thus the calculation result has deviated from the real value. It is hard to capture the actual mechanic behavior by numerical model.

In order to explain the difference between pre-swing defects and manufacturing defects on the joint buckling instability, the buckling simulation analysis of models with 1° and 3° pre-swing and 1° and 3° of manufacturing deviation, respectively, were carried out. The initial state of the flexible joint before swinging is shown in Figure 10.

The maximum pressure of 6 MPa was applied to calculate the swing angle under different pressures, as shown in Figure 11. The same trend of the buckling behavior of the joint was observed for the pre-swing defect and the manufacturing deviation defect; however, the instability caused by manufacturing deviation is more severe. This conclusion also confirms the deviation of the lateral force and the swing angle to be causes of high-pressure instability of the joint.

5. Container Pressure Torque

In order to apply the law of the spring torque variation under high pressure to industries, the actual swings of several kinds of flexible joints were analysed. It was found that the reduction of the spring torque under a certain pressure is the power function of the pressure compared with the initial spring torque, the order of which could be calibrated based on experimental data. Therefore, in this paper, we assume that a torque conducive to joint swing is produced by pressure when the flexible joint begins to swing. This torque, which we call the container pressure torque M_R, is significantly affected by the pressure. Assume that the sum of the spring torque M_τ^p under a certain pressure and M_R equals the initial spring torque M_τ^0. The relation between them could be written as follows:

$$M_R = M_\tau^0 - M_\tau^p. \tag{2}$$

Based on the experimental data for several different types of flexible joints and engineering experiences, the equation

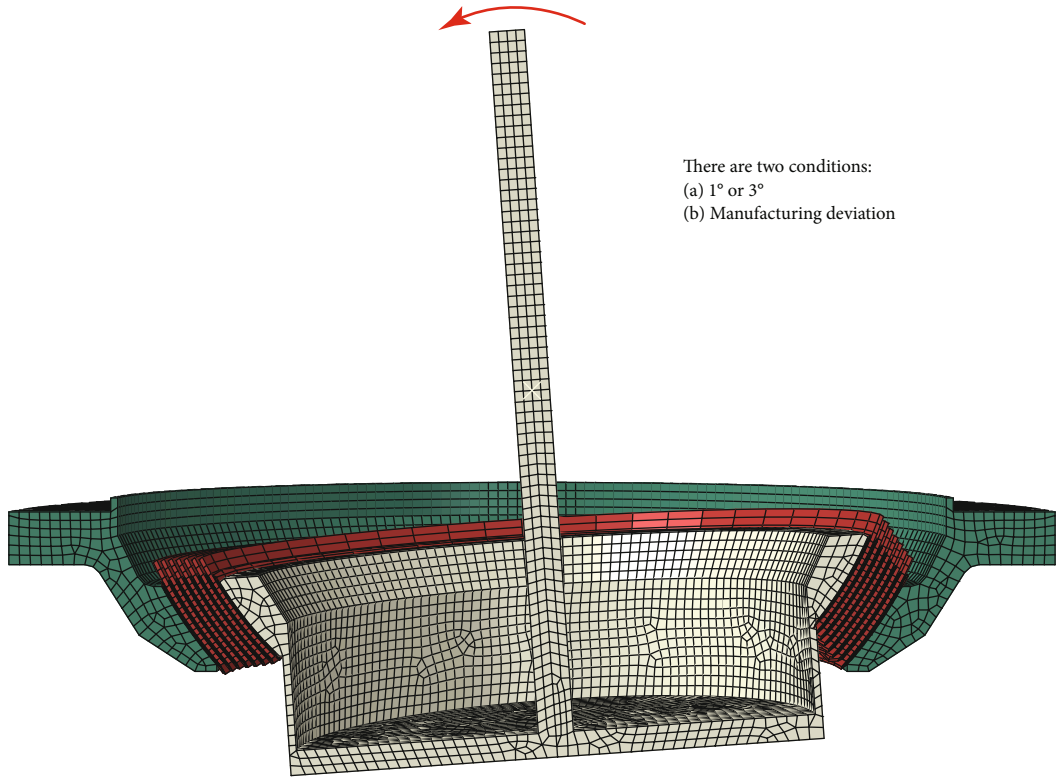

Figure 10: Initial state before the flexible joint is swung (there are two conditions: (a) the flexible joint rotates by 1 degree or 3 degrees of swing angle; (b) the 1- or 3-degree swing angle produced by the manufacturing error).

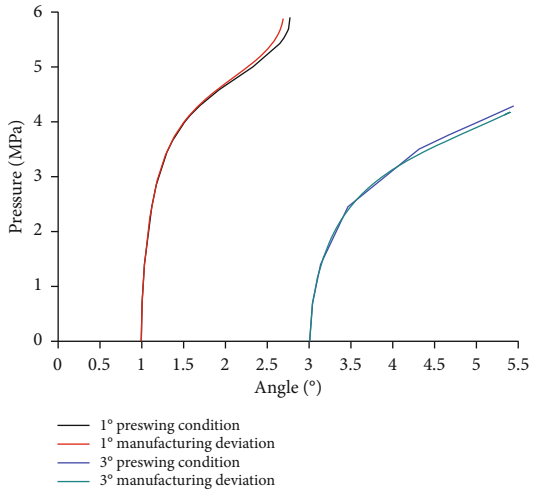

Figure 11: The influence of pre-swing and manufacturing deviation on swing angle.

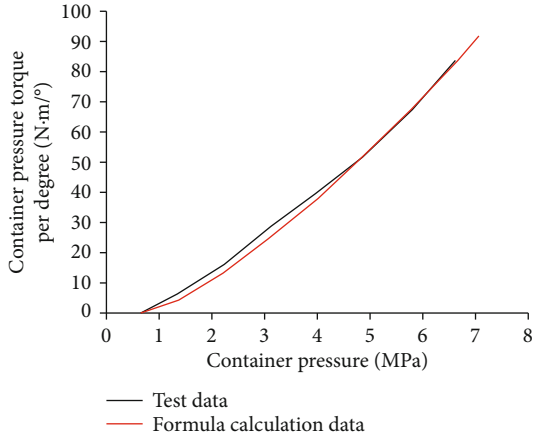

Figure 12: Joint number 1.

for calculating the ratio of container pressure torque to the initial spring torque was derived for flexible joints.

$$\frac{M_R}{M_\tau^0} = 1 - \frac{M_\tau^p}{M_\tau^0} = \left(\frac{P}{P_{cr}}\right)^k = \left(\frac{P_c - P_0}{(at_r/t_e{}^2 - n)(\beta_2 - \beta_1/\tan\beta)G}\right)^{2+\sin^2\varphi-\sin^2\beta}. \quad (3)$$

P_{cr} is the critical container pressure, which could be expressed as $P_{cr} = \mu G$ and is determined by the dimensions and elastic materials of the flexible joint. This means different P_{cr} values for different joints. μ is a shape factor.

P is the relative pressure, expressed as $P = P_c - P_0$, and could be calculated by differentiating the current pressure P_c and the initial pressure P_0 (0.2 MPa or 0.15 MPa). k is a pressure index, $k = 2 + \sin^2\varphi - \sin^2\beta$; α is the slewing radius of the joint, t_e is the thickness of the elastic rubber components, t_r is the thickness of the reinforcing component, ϕ is the cone angle, G is the shear torque of the

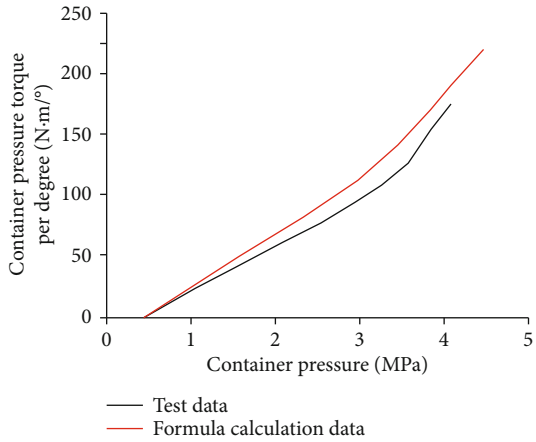

Figure 13: Joint number 2.

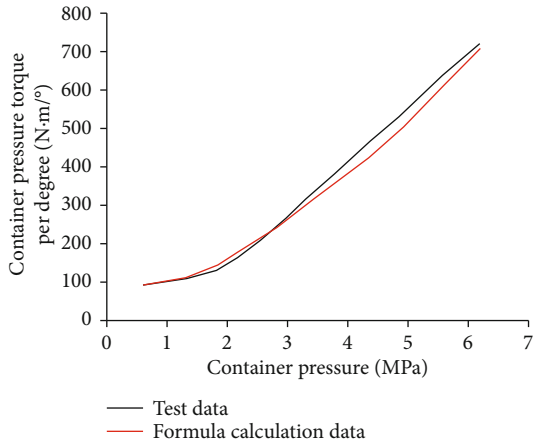

Figure 14: Joint number 3.

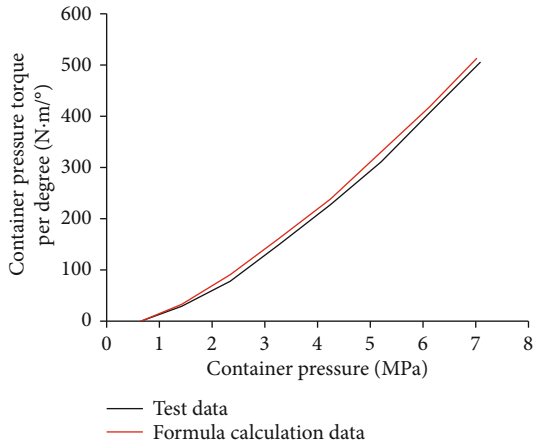

Figure 15: Joint number 4.

elastic rubber material, β is the joint angle, and β_1 and β_2 are the inner and outer joint angle, respectively.

To verify the accuracy of this equation, container pressure torque was calculated for several types of flexible joints at different pressures and was compared with the data from the swing test, as shown in Figures 12–15. Good alignment of the container pressure torque and the experimental data is achieved, and it could be thus used as guidance in the actual project.

6. Conclusions

In this study, the buckling characteristics of the flexible joint were analysed by simulating the pressure under the pre-swing flexible joint with different calculation methods. After comparing with the experimental results, the following conclusions are achieved:

(1) The root cause of the spring torque reduction of flexible joint under high pressure is the buckling response of flexible joint under swing torque and pressure. The deflection torque of joint is equivalent to the initial disturbance of the lateral force, which makes a certain angular displacement of the joint. As the pressure increases, the same torque will produce greater swing angular displacement, which means the spring torque will decrease

(2) Both the general and Riks methods can well simulate the swing instability of the joint, and the general method has a larger path-tracking range, which could be used to calculate the result under higher pressure. Through the simulation with the two methods, it was discovered that the buckling process of the flexible joint is the stable buckling process, but the exact buckling critical load of the flexible joint could not yet be captured via the numerical simulation method. Compared with the experimental results, the numerical results agree well with the experimental results with relatively small errors. Both of these methods can simulate the buckling behaving of flexible joints by force and thus could be used to pre-optimize the design of flexible joints

(3) By comparing the effects of the manufacturing bias (such as uneven thickness of the elastic rubber components) and the pre-swing angle on the buckling of the joint, it was discovered that the buckling instability of the joint in both cases is consistent, which explains the self-dumping of flexible joint during the actual pressurization experiment

(4) In order to facilitate the engineering application, this paper puts forward the concept of container pressure torque and summarizes the calculation formula of this torque. The experimental data demonstrated the excellent accuracy of the calculation formula, which serves as a useful reference for the design of flexible joints

Data Availability

As most of the data in this manuscript were related to trade secrets, I cannot provide them completely. In the future, if necessary, I can share some data with the reviewers or readers.

Conflicts of Interest

The authors declare that they have no conflicts of interest.

Acknowledgments

This article was funded by Xi'an Modern Chemistry Research Institute, China.

References

[1] C. Ruxun, "Design and research of solid rocket motors," *Beijing: Astronautics Press*, pp. 260–320, 2007.

[2] W. Chunguang, S. Hongbin, W. Xuekun, L. Jiang, and S. Baolin, "Numerical analysis of deflection torque of flexible joint with high pressure," *Journal of Propulsion Technology*, vol. 32, no. 2, pp. 202–206, 2011.

[3] Z. Xiaoguang, L. Yu, R. Junxue, Y. Jingxian, and Y. Wei, "Performance test of thrust vector of small flexible joints," *Journal of Aerospace Power*, vol. 27, no. 12, 2012.

[4] W. Chao, R. Junxue, H. Wenqiang, L. Yu, and Y. Jingxian, "Characteristics of effective pivot point excursion for flexible joint," *Journal of Aerospace Power*, vol. 29, no. 12, pp. 2993–2999, 2014.

[5] S. Hongbin, G. Zhengxi, and H. Xiao, "Dynamic response study of flexible nozzle in solid rocket motor," *Journal of Aerospace Power*, vol. 18, no. 4, 2003.

[6] S. Shani, S. Putter, and A. Peretz, "Development of a high-performance flexible for thrust vector control," AIAA95-3047.

[7] J. R. Donat, "Solid rocket motor nozzle flex seal design sensitivity," AIAA93-1122.

[8] C. L. An and X. L. Chang, "Super-elasticity constitutive parameter fit and low-pressure wiggle nonlinear finite element analysis of flexible joint elastomer," *Journal of Solid Rocket Technology*, vol. 31, no. 1, 2008.

[9] C. Cuiwei, C. Weimin, C. Timin, and L. Min, "Structural analysis on solid rocket motor flexible joint," *Journal of Propulsion Technology*, vol. 27, no. 5, 2006.

[10] C. Cuiwei, C. Weimin, C. Timin, and L. Min, "Elastomer Anylisis on Flexible Nozzle of Solid Rocket Motor," *Aerospace Materials and Technology*, vol. 35, no. 5, 2005.

[11] W. Xuekun, W. Chunguang, and S. Hongbin, "Compression-shear-combined loading experiment studies and numerical analysis of flexible joint elastomer," *Journal of Solid Rocket Technology*, vol. 34, no. 3, pp. 364–368, 2011.

[12] C. Wang, T. Weiping, S. Hongbin, L. Jiang, C. Cong, and W. Chunguang, "Dependent of shear modulus of elastomer on different pressure," *Aerospace Materials and Technology*, vol. 41, no. 5, 2011.

[13] H. Qiang, "Dynamic buckling and branching of elastoplastic system," *Beijing: Science Press*, pp. 2–30, 2000.

[14] G. Alfano and M. A. Crisfield, "Solution strategies for the delamination analysis based on a combination of local-control arc-length and line searches," *International Journal for Numerical Methods in Engineering*, vol. 58, no. 7, pp. 999–1048, 2003.

[15] E. A. de Souza Neto and Y. T. Feng, "On the determination of the path direction for arc-length methods in the presence of bifurcations and 'snap-backs'," *Computer Methods in Applied Mechanics and Engineering*, vol. 179, no. 1-2, pp. 81–89, 1999.

[16] L. Wenguang, *Study on Mechanical Properties and Seismic Response Analysis of Rubber Isolation Bearings*, Beijing University of Technology, Beijing, 2003.